Quantum percolation in three-dimensional systems

C. M. Soukoulis

Ames Laboratory and Department of Physics, Iowa State University, Ames, Iowa 50011

Qiming Li

Department of Chemistry, Massachusetts Institute of Technology, Cambridge, Massachusetts 02139

Gary S. Grest

Corporate Research Science Laboratory, Exxon Research and Engineering Company, Annandale, New Jersey 08801

The quantum site- and bond-percolation problems, which are defined by a disordered tight-binding Hamiltonian with a binary probability distribution, are studied using finite-size scaling methods. For the simple-cubic lattice, the dependence of the mobility edge on the strength of the disorder is obtained for both the site- and bond-percolation case. We find that the quantum percolation threshold is $p_q^s = 0.44 \pm 0.01$ for the site case and $p_q^b = 0.32 \pm 0.01$ for the bond case. A detailed numerical study of the density of states (DOS) is also presented. A rich structure in the DOS is obtained and its dependence on the concentration and strength of disorder is presented.

I. INTRODUCTION

Considerable progress has been made in our understanding of the effects of disorder on the nature of the electronic wave functions.[1] It is now well established that for dimensions $d \geq 3$, there is a localization transition between extended and localized states, as the strength of the disorder increases. Complete localization is predicted for $d \leq 2$ by the one-parameter scaling theory. This scaling theory is supported by a larger number of numerical studies in $d = 2$ and 3. In recent years, interest has also focused on quantum percolation problems.[2-9] In the model of quantum percolation, a quantum-mechanical entity propagates through a lattice in which a certain fraction of sites or bonds have been blocked. This model can provide insight into the role of quantum effects in electron motion in disordered systems.

Quantum percolation is usually formulated in terms of a tight-binding one electron Hamiltonian,

$$H = \sum_n |n\rangle \varepsilon_n \langle n| + \sum_{\substack{n,m \\ (n \neq m)}} |n\rangle V_{nm} \langle m| , \qquad (1)$$

where the transfer energy V_{nm} vanishes unless n and m are nearest neighbors and $|n\rangle$ represents a wave function localized near site n. As in the classical case, one can define site and bond quantum percolation. In the site-percolation problem, the site energy ε_n is assumed to obey the distribution

$$P(\varepsilon_n) = p\delta(\varepsilon_n - \varepsilon_A) + (1-p)\delta(\varepsilon_n - \varepsilon_B), \quad \varepsilon_B = -\varepsilon_A \qquad (2)$$

where $\delta = |\varepsilon_A - \varepsilon_B|/zV = 2\varepsilon_A/zV$ determines the degree of disorder, z is the number of nearest neighbors, and $V_{nm} = V$ is a constant. In the bond-percolation problem, the site energies ε_n are constant, and may be arbitrarily taken to be zero, $\varepsilon_n = 0$, while the nearest neighbor

transfers energies V_{nm} are distributed according to

$$P(V_{nm}) = p\delta(V_{nm} - V) + (1-p)\delta(V_{nm} - V_B) , \qquad (3)$$

with $V_B = 0$. These probability distributions are essentially characterized by two parameters: p, the concentration of A atoms (bonds), i.e., the probability that a given site (bond) is occupied and ε_A (V). One important limiting case is that of the binary-alloy distribution where $\varepsilon_A \to \infty$ ($V_B \to 0$). In this case, the only way in which an electron initially at an A (B) site or a V bond may propagate across the sample is to find a path consisting entirely of A (B) sites or V bonds which percolates. Classical percolation theory examines exactly this problem, i.e., the probability of finding such a path which spans the sample. Sites with infinite site energy and bonds with zero transfer energy represent impediments for the motion of a quantum particle governed by the Schrödinger equation with the Hamiltonian in Eq. (1). One of the main concerns in quantum percolation problems is to locate the quantum percolation threshold, p_q, for the site and the bond case, below which all eigenstates of the Hamiltonian are localized It is clear that the quantum threshold must be greater than its classical counterpoint p_c, since the existence of an infinite cluster is a necessary but not sufficient condition for the existence of an extended state.

There has been a number of estimations[3-9] of the quantum percolation threshold for the site and the bond cases, both for the square and simple-cubic (sc) lattices. While all the different numerical methods clearly show that p_q is greater than p_c, there is no general agreement on the precise value of p_q for the site and bond cases, in the square and sc lattices. Numerical estimates[3-9] of quantum-site percolation thresholds range from 0.59 to 1.00 for the square and from 0.38 to 0.48 for the sc lattice. For comparison, we note that the classical site (bond) percolation thresholds[4] are 0.59 (0.50) for the

square lattice and 0.31 (0.25) for the sc lattice, respectively. The most recent calculations[4,6-8] with large size systems using the scaling hypothesis or related approaches, narrow the range of p_q to $0.42 \leq p_q^s \leq 0.48$, with $p_q^s = 0.44 \pm 0.01$ as the best estimate[7] for the quantum site-percolation threshold on the sc lattice. For quantum bond percolation, the thresholds range from 0.50 to 1.00 for the square lattice and from 0.30 to 0.55 for the sc lattice. More recent calculations[4,5] narrow this range to $0.30 \leq p_q^b \leq 0.39$ for the sc lattice. New numerical results presented here give $p_q^b = 0.32 \pm 0.01$ as the estimate for the quantum bond-percolation threshold on the sc lattice. For the square lattice recent detailed numerical studies[9] for very large systems give very strong, and we believe convincing, evidence that no localization transition occurs for any amount of disorder. That is, $p_q = 1.00$ for the quantum percolation threshold for the site as well as for the bond case in $d = 2$, in agreement with the scaling theory of localization and in disagreement with a recent speculation[5] that $p_q < 1$ in $d = 2$.

While the main concern in the quantum percolation problem has been to locate the quantum percolation threshold, there have been some studies[2,7,8] of the structure in the DOS. Most of the earlier work has been for the site percolation on the square lattice. For weak site disorder, the DOS remain a single band which is a uniformly stretched version of the unperturbed DOS. However, for strong disorder $\delta \gtrsim 2$, the single band splits into two bands centered approximately at $-\varepsilon_A$ and ε_A with widths approximately equal to $2zVp$ and $2zV(1-p)$.[10] Another very interesting[2,7] feature of the DOS is a delta function or very narrow spike in the center of the subband and gaps on both sides of the central spike in which no states are found as $\delta \to \infty$. The gap narrows and the central peak broadens as p is increased and finally the gap disappears for large concentrations. In contrasts to the site case, only a narrow spike at $E = 0$ and a gap around it is observed in the single band of the DOS for the bond case.

The purpose of the present paper is to present a detailed numerical study of the quantum percolation problem on the basis of the finite-site scaling methods[11-14] using the very reliable transfer-matrix technique. For the sc lattice we numerically calculated the entire mobility-edge trajectory in the concentration-energy plane for both the site- and bond-percolation problems.[5] We have also determined, numerically, the integrated density of state (DOS) for both cases which shows a very rich structure for the site case. In Sec. II, we briefly describe the formalism and the method of calculation. In Sec. III, we present and discuss the results of this calculation, and in the final section, we summarize the conclusions of this work.

II. METHODS OF CALCULATION

The most reliable numerical technique to obtain quantitative results for Anderson localization in disordered systems is the transfer-matrix method.[11-14] In this method, one considers coupled 1D systems. Each 1D system is described by a tight-binding Hamiltonian of the form given by Eq. (1). In this study, we assume that the probability distribution $P(\varepsilon_n)$ of the random sites and $P(V_{nm})$ of the random bonds are described by Eqs. (2) and (3), respectively. [In previous numerical calculations,[13,14] we have systematically studied the behavior of the tight-binding disordered systems when $P(\varepsilon_n)$ is given by either a rectangular or a Gaussian probability distribution.] The corresponding sites or bonds of the nearest-neighbor 1D system are coupled together by an interchain matrix element. In 2D, one studies systems of width M and length N, while in 3D the systems have a square cross sectional area of M^2. We use periodic boundary conditions in the direction(s) perpendicular to the axis of the 1D chains. For M regularly placed chains of length N, one determines the largest localization length λ_M as $N \to \infty$. From a plot of λ_M versus M, one can determine the localization properties of the system. The function λ_M versus M has two distinct branches. One corresponds to a localized state, in which the second derivative $d^2\lambda_M/dM^2$ is negative and λ_M approaches a finite value λ as $M \to \infty$, where λ is the localization length. The second branch corresponds to an extended state, in which $d^2\lambda_M/dM^2$ is positive and $\lambda_M \to \infty$ as $M \to \infty$. At exactly the mobility edge, we have found for a number of disordered tight-binding models, in 3D with a rectangular, Gaussian, or binary probability for the site energies, that $\lambda_M/M \simeq 0.6$. In our calculations, for quantum percolation in 3D, we have used systems with $M = 2-9$ and N was at least 6 000.

In addition to the localization length, we also calculated the integrated DOS; the Sturm sequence method was employed.[15,16] The method consists of an application of Gaussian elimination on the consecutive columns or rows of the matrix $(E\hat{1} - H)$, where E is the energy and $\hat{1}$ is a unit matrix of the same size as H given by Eq. (1). The Gaussian elimination of the elements of the matrix is applied until the matrix is reduced to a triangular form. The integrated DOS is then calculated by counting the fractional number of positive elements in the diagonal of the reduced triangular matrix. For details of the method, see Ref. 15. The advantage of using this method is both economy in storage and speed. The computing time increases as $M^{3(d-1)} \times N$, which allows one to study very long strips of length N of appreciable width M. It also does not require matrix inversion. In our calculations, we have used systems of size $10 \times 10 \times 400$ and $20 \times 20 \times 100$.

III. NUMERICAL RESULTS AND DISCUSSION

In this section, we present results based upon the numerical techniques discussed above. Here we consider the sc lattice and the probability distribution $P(\varepsilon_n)$ of the random sites and $P(V_{nm})$ of the random bonds are described by Eqs. (2) and (3), respectively. These probability distributions are essentially characterized by two parameters: p, the concentration of A atoms (bonds), i.e., the probability that a given site (bond) is occupied and $\varepsilon_A(V)$. For the site-percolation case $\delta = 2\varepsilon_A/zV$ can be considered as determining the degree of disorder. One important limiting case is that of the binary alloy, in which $\varepsilon_A \to \infty$ ($V_B \to 0$). In this case, the only way an

electron initially at an A (B) site or a V bond can propagate across the sample is on a path consisting entirely of A (B) sites or V bond which percolates. Therefore, sites with infinite site energy and bonds with zero transfer energy represent blocks for the motion of a quantum particle governed by the Schrödinger equation with the Hamiltonian in Eq. (1). Accordingly, the quantum percolation threshold p_q, above which all eigenstates of the Hamiltonian are extended, must be greater than its classical counterpart p_c. The existence of an infinite cluster is a necessary but not a sufficient condition for the existence of an extended state. We have systematically calculated the λ_M's for several values of p, energy E as $\delta \to \infty$ ($V_B \to 0$) for the (bond-) percolation problem. For the site problem, we have chosen $\varepsilon_A \geq 60$, i.e., $\delta \geq 2\varepsilon_A / zV = 20$ and the energy E is measured from the center of the A subband, i.e., $E = 0$ in the site problem corresponds to $E = \varepsilon_A$, if not otherwise specified. For the bond problem, we used the probability distribution given by Eq. (3) with $V = 1$. V_B was taken to be a very small nonzero value since for finite M, there is always a finite probability that the system would break into several disconnected pieces. Our results were independent of the value of V_B, provided that $V_B \leq 10^{-4}$. In Fig. 1(a), we present the results of the mobility-edge trajectory for the

site case in the concentration-energy plane. The energy shown in Fig. 1(a) is measured from the center of the A subband, i.e., $E = 0$, corresponds to $E = \varepsilon_A$. Only the mobility-edge trajectory for $E \geq 0$ is shown, since it is symmetric around $E = 0$. It was previously shown[7] that the quantum-site percolation threshold p_q is a very sensitive function of the strength of the disorder ε_A for $E = 0$, while there is a much weaker dependence on ε_A for $E \neq 0$. At the center of the A subband ($E = 0$) p_q is most probably equal to 1 in the limit $\varepsilon_A \to \infty$, as was first suggested by Kirkpatrick and Eggarter.[2] As can be seen from Fig. 1(a), the lowest value of the quantum-site percolation threshold is $p_q^s = 0.44 \pm 0.01$ and occurs for an energy near the center of the subband. Notice that in the region $E / 2V \leq 1$, p_q is nearly constant with the exception of the sharp peak at $E = 0$ and a weak maximum at $E / 2V \simeq 0.5$. In Fig. 1(b), we present the results for the mobility-edge trajectory for the bond case in the concentration-energy plane. The shape of the mobility-edge trajectory for the bond case is very similar to the one, shown in Fig. 1(a), for the site case. Notice that in the region $E / 2V \leq 1$, p_q is also nearly constant with the exception of the sharp peak at $E = 0$ and a weak maximum at $E / 2V \simeq 0.5$. As can be seen from Fig. 1(a), the lowest value of the quantum bond-percolation threshold is $p_q^b = 0.32 \pm 0.01$ in good agreement with previous numerical work.[4,5] We believe that the transfer-matrix method gives a better estimate, since it has been tested in a number of other cases.[11-14] In Ref. 7, we have also compared the mobility-edge trajectory for the site-percolation problem obtained by the transfer-matrix technique with the predictions of the potential well analogy[14] based on a cluster coherent potential approximation. The agreement is satisfactory.

Now let us consider some properties of the DOS. For the site-percolation problem, for a given p and δ or ε_A the DOS has the following form. For zero disorder, $\delta = \varepsilon_A = 0$, there is a single band from $E = -6V$ to $6V$ for the simple-cubic lattice. As the disorder increases the DOS remains a single band which is a uniformly stretched version of the unperturbed DOS. For stronger disorder $\delta \gtrsim 2$, this single band splits into two bands centered approximately at $-\varepsilon_A$ and ε_A with widths equal to $2zVp$ and $2zV(1-p)$. CPA results[10,17] show this behavior as well as some numerical results.[2,7] Another very interesting feature of the DOS is a δ-function spike in the center of the subband and gap regions on both sides of the central spike in which no states are found[2,7] for $\delta \to \infty$. The width of the gap narrows and the central spike broadens as the concentration is increased. Finally, for larger concentrations there is no structure (either a central spike or a dip) in the DOS around $E = 0$.

Here we present a systematic study of the DOS. We found an unusually rich structure in the DOS. In Fig. 2, we plot the exact[10] and the numerically calculated band-edge limits of the DOS for the 3D site-percolation problem. Here we have used $p = 0.10$ as a typical case. For this concentration, CPA results[10] already exist and therefore we are able to compare our results with them. We plot $\delta = 2\varepsilon_A / 6V$, which is proportional to the strength of
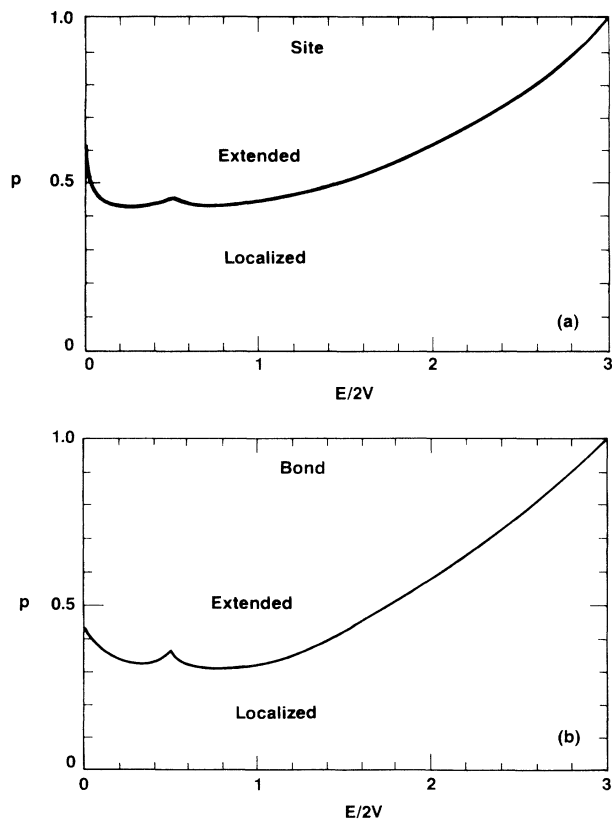

FIG. 1. Mobility-edge trajectory in the concentration-energy plane for the sc lattice for the site (a) and bond (b) quantum percolation model. In (a) the energy is measured from the center of the A subband, i.e., $E = 0$, corresponds to $E = \varepsilon_A$.
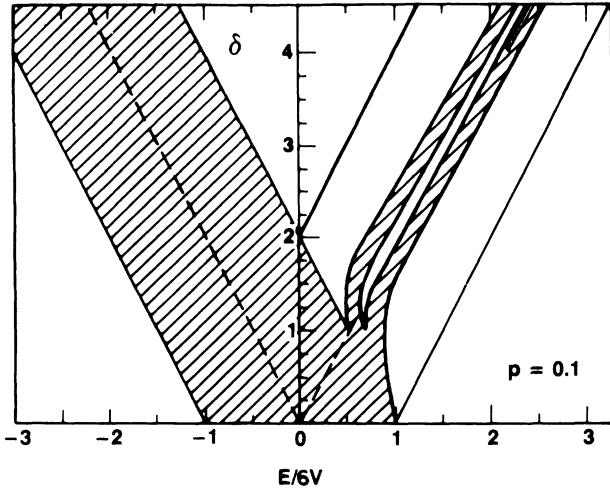
FIG. 2. The exact and the numerically calculated DOS limits of the density of states for the site-percolation problem in an sc system for $p = 0.10$ vs $\delta = 2\varepsilon_A/6V$. The shaded area is the band. The dashed line denotes the site energies ε_A ($E > 0$) and $-\varepsilon_A$ ($E < 0$).

merically calculated DOS limits is given. Traditionally, the DOS of disordered systems is obtained through the application of the CPA. Since the CPA is an approach based on an effective periodic medium, it is not able to describe the effects due to the local environment of the atoms, and then it cannot reproduce the peaked structure of the minority subband. Due to this problem, there have been a number of attempts to generalize the CPA to include the cluster effects.[10] In Fig. 3, both ε_A and E are given in units of V. Notice that for small values of ε_A there are no gaps around $E = \varepsilon_A$. However, as ε_A increases a gap develops first to the right of the $E = \varepsilon_A$ line, which eventually moves to the left of the $E = \varepsilon_A$ line. As

the disorder versus energy. The solid lines originating from ($\delta = 0$, $E = \pm 6V$) and from ($\delta = 2$, $E = 0$) are the exact band-edge trajectories in $\delta - E$ plane. One expects[10] that a gap must open up when $\delta > 2$. However, as one can see from Fig. 2, this is not the case. Our detailed numerical results show that the band splits when the strength of the disorder $\delta \gtrsim 1$. Similar behavior has been seen in the CPA calculations.[10] In addition, our numerical results show that there is a rich structure in the DOS of the minority subband not observed previously. In Fig. 2, one can clearly see that there is a gap to the left of the center of the minority subband. As δ increases to higher values, $\delta \gtrsim 4$, another gap to the right of the center of the minority subband appears. This rich structure is clearly shown in Fig. 3, where the detailed structure of the nu-
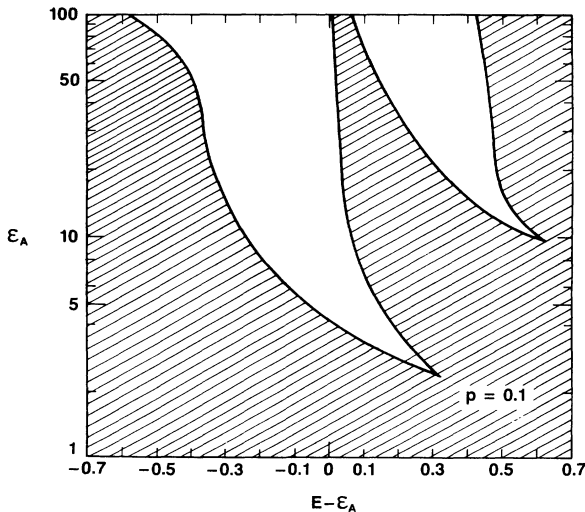

FIG. 3. A detailed structure of the numerically calculated DOS limits of the site-percolation problem in a simple-cubic system for $p = 0.10$. The site energy ε_A and E are given in units of V. The shaded area is the band.
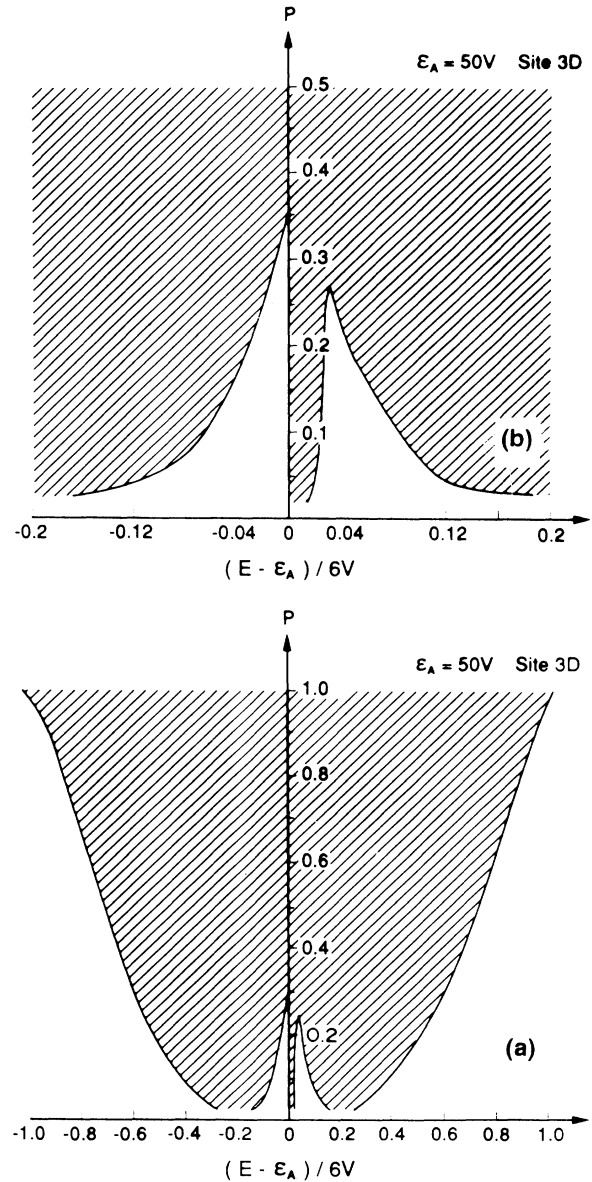

FIG. 4. (a) The band-edge structure of the site-percolation problem is a simple-cubic system for $\varepsilon_A = 50$ V ($\delta = 16.67$). (b) A detailed picture of the band-edge structure for concentration $p \lesssim 0.5$. The shaded area is the band in both (a) and (b).

ε_A increases further, $\varepsilon_A \gtrsim 10$, a second gap appears to the right of the $E = \varepsilon_A$ line. Notice that for very high values of ε_A, $\varepsilon_A > 100$, a spike develops at $E = \varepsilon_A$ and gap regions on both sides of $E = \varepsilon_A$ appear. The structure in the DOS shown in Figs. 2 and 3 is for $p = 0.10$. To understand how the band-edge trajectories change as a function of the concentration p, we have chosen $\varepsilon_A = 50$ V, as a typical case, and numerically calculate the DOS band-edge limits. The results are shown in Fig. 4. We only give the band and the gap structure around the center of the A subband, $E = \varepsilon_A$. Notice for low values of p, $p \lesssim 0.35$, there is significant structure in the DOS. A gap is present on both sides of the center of the A subband. As p increases, one sees that the gaps become narrower and eventually disappear when $p \gtrsim 0.35$. In Figs. 4(a) and 4(b), the DOS shows an obvious central spike at the center of the subband and a gap region of energy on both sides of the central spike in which no states are found. When the concentration p is increased, both the strength of the central spike as well as the gaps around it decrease. Finally, in very high concentrations the gap around $E = \varepsilon_A$ is no longer apparent. In Fig. 4, we only present the band-edge trajectories of the DOS and not their weight. In order to find out how many states the spike around $E = \varepsilon_A$ contains, we have also calculated the integrated DOS around the central spike. In Fig. 5, we plot the percentage P_I of the number of states in the central spike of the DOS for the 3D site-percolation problem versus the concentration p. P_I is defined as the integrated DOS around the central spike of the DOS divided by p. Notice that the percentage of the number of states in the central spike decreases as p increases. The origin of the central spike around $E = 0$ is due to isolated single sites and odd numbers of sites. The probability of such an occurrence can be calculated[2] as a function of p. This seems to agree reasonably well with the results of the percentage of the number of states in the central spike versus p shown in Fig. 5. For low p, the central spike contains a large number of states with two well defined gaps around it. For example, when $p = 0.20$, the percentage of the number of states in the central spike is
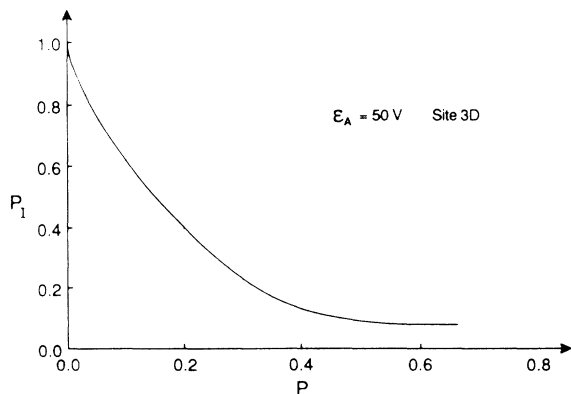

FIG. 6. Density-of-states histogram for the 3D bond-percolation problem for $p = 0.35$. In the inset, details of the DOS very close to $E \simeq 0$ are shown. Since the DOS is symmetric around $E = 0$, only the results for $E > 0$ are given.

8%, while for $p = 0.60$, the percentage is only 5%.

For the bond-percolation problem, we have also calculated the DOS. In Fig. 6, we present the results of the DOS versus E for the 3D bond-percolation problem for $p = 0.35$. Note that there is also a spike at $E = 0$, with gaps around $E = 0$. This is clearly seen in the inset of Fig. 6. There is also a peak close to $E/6V = 0.18$. This peak is due to single isolated bonds existing in this structure. As the concentration increases, the strength of the central spike decreases and the width of the gaps around $E \simeq 0$ become narrower. As p $(p \gtrsim 0.6)$ increases, the gaps around $E = 0$ disappear, and there is no central spike. Finally in Fig. 7, we plot the percentage of the number of states in the central spike of the DOS for the 3D bond-percolation problem versus p. Note that P_I decreases rapidly as p increases and goes to zero for $p \gtrsim 0.6$. In contrast to the site case, this dependence can be explained only qualitatively by the probability of having small numbers of sites with $E \simeq 0$.

FIG. 5. The percentage P_I of the number of states in the central spike of the DOS for the 3D site-percolation problem vs the concentration p. P_I is defined as the integrated DOS around the central spike of the DOS divided by the concentration p.
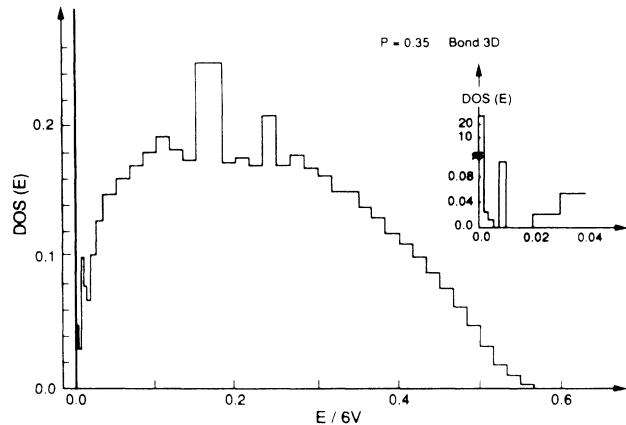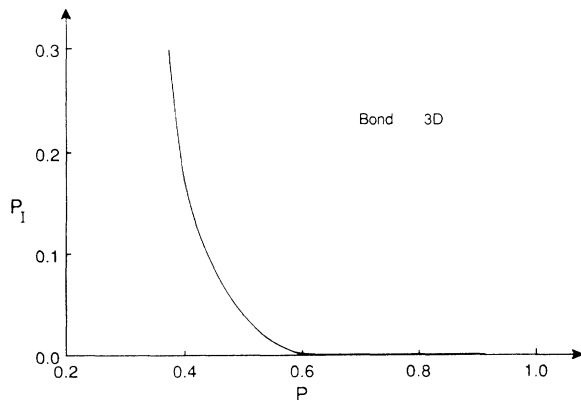

FIG. 7. The percentage P_I of the number of states in the central spike of the DOS for the 3D bond-percolation problem vs the concentration p.

IV. CONCLUSIONS

In conclusion, we have calculated the quantum site- and bond-percolation thresholds on an sc lattice not only at the center of the subband as in previous studies, but for the entire energy region. The quantum percolation threshold is determined to be 0.44±0.01 for the site problem and 0.32±0.01 for the bond problem. We have also carried out a detailed numerical study of the structures of the DOS for the site- and bond-percolation problems. A very interesting feature of the DOS is an obvious δ-function spike in the center of the subband and gap regions on both sides of the central spike in which no states are found. A detailed study of the dependence of the strength of the central spike of the DOS, as well as of the width of the gaps around it as a function of the concentration p, was presented. The width of the gap narrows and the central spike broadens as the concentration p is increased. For larger concentrations, there is no structure (either a central spike or a dip) in the DOS around $E \simeq 0$.

[1] For a recent review see, e.g., Physica A **167**, 1 (1990).

[2] S. Kirkpatrick and T. P. Eggarter, Phys. Rev. B **6**, 3598 (1972).

[3] R. Raghavan, Phys. Rev. B **29**, 784 (1984); S. N. Evangelou, *ibid.* **27**, 1397 (1983); V. Srivastava and M. Chaturvedi, *ibid.* **30**, 2238 (1984).

[4] T. Odagaki and K. C. Chang, Phys. Rev. B **30**, 1612 (1984); K. C. Chang and T. Odagaki, J. Phys. A **20**, L1027 (1987).

[5] Y. Shapir, A. Aharony, and A. B. Harris, Phys. Rev. Lett. **49**, 486 (1982); Y. Meir, A. Aharony, and A. B. Harris, *ibid.* **56**, 976 (1986); Europhys. Lett. **10**, 275 (1989).

[6] L. J. Root, J. D. Bauer, and J. L. Skinner, Phys. Rev. B **37**, 5518 (1988); L. J. Root and J. L. Skinner, *ibid.* **33**, 7738 (1986).

[7] C. M. Soukoulis, E. N. Economou, and G. S. Gret, Phys. Rev. B **36**, 8649 (1987).

[8] Th. Koslowski and W. von Niessen, Phys. Rev. B **42**, 10 342 (1990).

[9] C. M. Soukoulis and G. S. Grest, Phys. Rev. B **44**, 4685 (1991).

[10] R. J. Elliot, A. J. Krumhansl, and P. L. Leath, Rev. Mod. Phys. **46**, 437 (1974), and references therein.

[11] J. L. Pichard and G. Sarma, J. Phys. C **14**, L127 (1981); **14**, L617 (1981); **18**, 3457 (1985).

[12] A. Mackinnon and B. Kramer, Phys. Rev. Lett. **47**, 1546 (1981); Z. Phys. B **53**, 1 (1983); B. Bulka, B. Kramer and A. Mackinnon, *ibid.* **60**, 13 (1985); B. Bulka, M. Schreiber, and B. Kramer, *ibid.* **66**, 21 (1987).

[13] C. M. Soukoulis, I. Webman, G. S. Grest, and E. N. Economou, Phys. Rev. B **26**, 1838 (1982).

[14] E. N. Economou, C. M. Soukoulis, and A. D. Zdetsis, Phys. Rev. B **30**, 1686 (1984); A. D. Zdetsis, C. M. Soukoulis, E. N. Economou, and G. S. Grest, *ibid.* **32**, 7811 (1985); C. M. Soukoulis, A. D. Zdetsis, and E. N. Economou, *ibid.* **34**, 2253 (1986).

[15] *The Recursion Method and its Applications,* edited by D. G. Pettifor and D. L. Weaire, Springer Tracks in Modern Physics Vol. 58 (Springer-Verlag, Berlin, 1985); P. Dean, Rev. Mod. Phys. **44**, 127 (1972).

[16] Qiming Li, C. M Soukoulis, and E. N. Economou, Phys. Rev. B **37**, 8289 (1988).

[17] D. C. Licciardello and E. N. Economou, Phys. Rev. B **11**, 3697 (1975).